

Are your **MRI contrast agents** cost-effective?

Learn more about generic **Gadolinium-Based Contrast Agents**.



**AJNR**

**Iron and Volume in the Deep Gray Matter:  
Association with Cognitive Impairment in  
Multiple Sclerosis**

C.M. Modica, R. Zivadinov, M.G. Dwyer, N. Bergsland,  
A.R. Weeks and R.H.B. Benedict

This information is current as  
of April 20, 2024.

*AJNR Am J Neuroradiol* published online 19 June 2014  
<http://www.ajnr.org/content/early/2014/06/19/ajnr.A3998>

# Iron and Volume in the Deep Gray Matter: Association with Cognitive Impairment in Multiple Sclerosis

C.M. Modica, R. Zivadinov, M.G. Dwyer, N. Bergsland, A.R. Weeks, and R.H.B. Benedict

## ABSTRACT

**BACKGROUND AND PURPOSE:** There is a well-established correlation between deep gray matter atrophy and cognitive dysfunction in MS. However, the cause of these signs of neurodegeneration is poorly understood. Iron accumulation in the deep gray matter is higher in patients with MS compared with age- and sex-matched healthy controls, and could contribute to disease progression. Our objective was to evaluate the relationship between iron and cognition in several deep gray matter structures while accounting for the influence of volume loss.

**MATERIALS AND METHODS:** Eighty-five patients with MS and 27 healthy volunteers underwent 3T MR imaging and neuropsychological examination. We used SWI filtered phase to analyze the mean phase of low-phase voxels, indicative of abnormal iron accumulation.

**RESULTS:** Correlations between mean phase of low-phase voxels and cognitive tests were found in the caudate nucleus ( $r = 0.240$  and  $0.232$ ), putamen ( $r = 0.368$ ,  $0.252$ , and  $0.238$ ), globus pallidus ( $r = 0.235$ ), and pulvinar nucleus of thalamus ( $r = 0.244$ ,  $0.255$ , and  $0.251$ ) ( $P < .05$ ). However, correlations between structure volume and cognition were more robust. Furthermore, the introduction of structure volume into hierarchical regression analyses after iron metrics significantly improved most models, and mean phase of low-phase voxels did not account for significant variance after volume.

**CONCLUSIONS:** These findings suggest that iron accumulation plays a significant, if minor, role in MS cognitive decline.

**ABBREVIATIONS:** BVMT-R = the total learning portion of the Brief Visuospatial Memory Test-Revised; CVLT2 = total learning portion of the California Verbal Learning Test; DGM = deep gray matter; DKEFS-CS = Delis-Kaplan Executive Function System Sorting Test; LPV = low-phase voxel; MP-LPV = mean phase of the low-phase voxels; NP = neuropsychological; PASAT = 3-second Paced Auditory Serial Addition Test; SDMT = Symbol Digit Modalities Test

Investigation of iron accumulation in the central nervous system is an emerging area of research. Iron is elevated in MS at the areas of demyelination<sup>1</sup> and in the CSF,<sup>2</sup> and could potentially contribute to the understanding of progressive neurodegenerative disease. Iron deposition may adversely impact cellular function, such as enhancing or decreasing production of proteins, or it can cause oxidative stress leading to cell death, directly causing structural damage in the brain.<sup>3</sup>

SWI is an available method that estimates the degree of iron

deposition, in vivo, using MR imaging.<sup>4</sup> In a study examining the deep gray matter (DGM) of patients with MS, low-phase voxel (LPV) analysis reflected increased iron accumulation in the caudate nucleus, putamen, globus pallidus, and pulvinar.<sup>5</sup> Even in clinically isolated syndrome, this representation of increased iron accumulation was found in the putamen and pulvinar.<sup>6</sup> In a pediatric MS cohort, analysis of LPV reflected increased iron accumulation in both the thalamus and pulvinar while the volume of the LPV was increased in the pulvinar.<sup>7</sup> LPV volume was also increased in clinically isolated syndrome in the caudate nucleus, putamen, and pulvinar,<sup>6</sup> and magnetic susceptibility (also indicative of iron level) was increased in the caudate nucleus, putamen, globus pallidus, and pulvinar.<sup>8</sup>

Contemporary research shows that brain atrophy is predictive of cognitive disability in MS, more so than lesion burden.<sup>9,10</sup> GM atrophy is the subject of intense research because of its correlation with disease progression, neurologic disability,<sup>11</sup> cognitive impairment, and neuropsychiatric symptoms.<sup>12</sup> Regional analysis of the DGM in MS revealed that volume is reduced in the thalamus, caudate nucleus, putamen, and globus pallidus.<sup>13,14</sup> Likewise,

Received March 28, 2014; accepted after revision April 7.

From the Neuroscience Program (C.M.M.), Buffalo Neuroimaging Analysis Center (C.M.M., R.Z., M.G.D., N.B., R.H.B.B.), MR Imaging Clinical Translational Research Center (R.Z.), and Department of Neurology (R.Z., R.H.B.B.), School of Medicine and Biomedical Sciences, and School of Public Health and Health Professions (A.R.W.), University at Buffalo, State University of New York, Buffalo, New York; and IRCCS (N.B.), "S. Maria Nascente," Don Gnocchi Foundation, Milan, Italy.

This study was supported in part by National MS Society grant #RG4060A3/1 awarded to R.H.B. Benedict.

Please address correspondence to Ralph H.B. Benedict, PhD, SUNY Buffalo Neurology, 100 High St, Suite E2, Buffalo, New York 14203; e-mail: benedict@buffalo.edu

<http://dx.doi.org/10.3174/ajnr.A3998>

**Table 1: Demographic characteristics, neuropsychological test scores, and mean phase of the low-phase voxels across subcortical deep gray matter structures**

	MS (n = 85)	NC (n = 27)	P Value
<b>Characteristics</b>			
Age	46.0 ± 9.2	41.9 ± 10.7	NS <sup>a</sup>
Education	14.4 ± 2.2	15.3 ± 2.4	NS <sup>a</sup>
Female, n (%)	59 (69.4)	17 (63.0)	NS <sup>a</sup>
Caucasian, n (%)	73 (85.9)	24 (88.9)	NS <sup>a</sup>
Right-handed, n (%)	77 (90.6)	25 (92.6)	NS <sup>a</sup>
Impaired, n (%)	52 (61.2)	1 (3.7)	<.001 <sup>a</sup>
Disease duration	10.9 ± 7.6		
DMT duration <sup>b</sup>	3.8 ± 3.6		
EDSS <sup>c</sup>	3.6 ± 1.9		
T2 lesion volume	18.5 ± 20.3		
T1 lesion volume	3.4 ± 7.1		
<b>NP test scores</b>			
SDMT	50.8 ± 15.8	66.0 ± 10.5	<.001 <sup>d</sup>
PASAT	42.0 ± 15.7	49.8 ± 8.7	.017 <sup>d</sup>
DKEFS-CS	9.5 ± 3.0	11.7 ± 2.4	<.001 <sup>d</sup>
CVLT2	52.1 ± 13.1	64.4 ± 7.4	<.001 <sup>d</sup>
BVMT-R	7.8 ± 2.8	10.4 ± 1.5	<.001 <sup>d</sup>
<b>MP-LPV</b>			
Thalamus	-0.099 ± 0.016	-0.092 ± 0.011	.027 <sup>a</sup>
Caudate nucleus	-0.178 ± 0.021	-0.166 ± 0.011	.007 <sup>a</sup>
Putamen	-0.184 ± 0.033	-0.172 ± 0.028	NS <sup>a</sup>
Globus pallidus	-0.195 ± 0.036	-0.179 ± 0.029	NS <sup>a</sup>
Pulvinar	-0.157 ± 0.036	-0.139 ± 0.012	.014 <sup>a</sup>

**Note:**—NC indicates healthy control; DMT, disease-modifying therapy; EDSS, Expanded Disability Status Scale; NS, not significant.

<sup>a</sup> P value is based on 1-way ANOVA.

<sup>b</sup> n = 68 for calculation of DMT duration as only 68 were on therapy.

<sup>c</sup> n = 83 for calculation of mean EDSS as 2 patients were not assessed during their clinical visit.

<sup>d</sup> P value is based on 1-way ANCOVA, controlling for age and years of education. Age, education, disease duration, and DMT duration data are given as mean years ± SD. Lesion volume is given as mean milliliters ± SD. NP test data for the SDMT, PASAT, DKEFS-CS, CVLT2, and BVMT-R are given as mean test score ± standard deviation. MP-LPV data in the thalamus, caudate nucleus, putamen, globus pallidus, and pulvinar structures are given as radians ± SD.

lower thalamus volume is found in clinically isolated syndrome,<sup>15</sup> and both whole thalamus and pulvinar volume are decreased in patients with pediatric onset.<sup>16</sup> DGM volumes are strongly correlated with fatigue<sup>17</sup> and performance on cognitive tests.<sup>13,14</sup> Total DGM volume was the strongest predictor of Expanded Disability Status Scale scores in a study utilizing various MR imaging metrics; LPV analysis, reflecting iron accumulation in the DGM, further increased the percentage of variance in the regression model.<sup>18</sup>

In sum, the literature shows that DGM atrophy is strongly associated with cognitive dysfunction in MS.<sup>13</sup> However, the role of iron deposition, as observed with SWI-filtered phase, in explaining cognitive dysfunction is less clear, and potentially interactive effects of iron and volume have not been explored. Here we present findings from an initial investigation of the relationship of iron deposition and cognitive ability in patients with MS.

## METHODS

### Participants

We studied 85 patients with clinically definite MS<sup>19</sup> and 27 healthy, demographically matched controls (Table 1) with approval from the Institutional Review Board. These subjects were a subset from a previously published cohort, and informed consent was obtained.<sup>12,13</sup> Patients were excluded from the study if they had previous or current substance abuse, current or past major medical, neurologic, or psychiatric disorder outside of MS, or if they had a relapse or steroid pulse treatment within 8 weeks before

evaluation. Patients with depressive disorders that emerged after MS onset were permitted, but those meeting criteria for current major depressive episode were excluded. Participants were free of developmental delay and any medical history that could potentially impact cognitive ability. Of the patients with MS, 57 (67.1%) were in relapsing-remitting, and 28 (32.9%) were in secondary-progressive disease course. Sixty-eight (80.0%) patients with MS were on disease-modifying therapy at the time of the study. Therapy included intramuscular interferon beta-1a, 44 mcg subcutaneous interferon beta-1a, natalizumab, glatiramer acetate, mycophenolate mofetil, intravenous immunoglobulin, interferon beta-1b, mitoxantrone, and the following combinations: intramuscular interferon beta-1a + mycophenolate mofetil, 22 mcg + 44 mcg subcutaneous interferon beta-1a, and glatiramer acetate + mycophenolate mofetil.

### MR Imaging Acquisition and Analysis

Participants were examined on a 3T Signa Excite HD 12.0 Twin Speed 8-channel scanner (GE Healthcare, Milwaukee, Wisconsin) with a maximum slew rate of 150 T/m/s and maximum gradient amplitude in each orthogonal plane of 50 mT/m. A multichannel head and neck coil (GE Healthcare) was used to acquire: 2D multiplanar dual FSE proton density and T2WI; FLAIR; 3D high-resolution T1WI using a fast-spoiled gradient echo with magnetization-prepared inversion recovery pulse and spin-echo T1WI; and SWI. Scans were acquired in an axial-oblique orientation, parallel to the subcallosal line. One average was used for all pulse sequences. With the exception of SWI, all sequences were acquired with a 256 × 192 matrix (frequency × phase), FOV of 25.6 cm × 19.2 cm (256 × 256 matrix with phase FOV = 0.75), for an in-plane resolution of 1 mm × 1 mm. For all 2D scans (proton density/T2, FLAIR, spin-echo T1), we collected 48 contiguous, 3-mm-thick sections. For the 3D high-resolution inversion recovery–fast-spoiled gradient echo, we acquired 180 1-mm-thick locations. Other relevant parameters were: for dual FSE proton density/T2, TE1/TE2/TR = 9/98/5300 ms, echo-train length = 14; for FLAIR, TE/TI/TR = 120/2, 100/8, 8500 ms, echo-train length = 24; spin-echo T1WI, TE/TR = 16/600 ms; for 3D high-resolution T1WI, TE/TI/TR = 2.8/900/5.9 ms, flip angle = 10°. SWI was acquired using a 3D flow-compensated gradient-echo sequence with 64 contiguous, 2-mm-thick sections, a 512 × 192 matrix, FOV = 25.6 cm × 19.2 cm (512 × 256 matrix with phase FOV 0.75), for an in-plane resolution of 0.5 mm × 1 mm, flip angle = 12°, and TE/TR = 22/40 ms.

T2 and T1 lesion volume was measured using a semiautomated edge detection contouring technique as previously de-

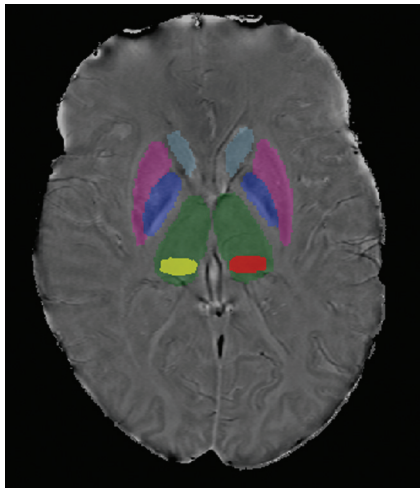


**FIG 1.** Scan demonstrating deep gray matter structure segmentation. FMRIB's Integrated Registration and Segmentation Tool was applied to the 3D high-resolution T1WI to segment the DGM. Pulvinar (yellow and red) was segmented using a semiautomated contouring technique.

scribed.<sup>20</sup> To segment the thalamus, caudate nucleus, putamen, and globus pallidus, FMRIB's Integrated Registration and Segmentation Tool<sup>21</sup> (<http://www.fmrib.ox.ac.uk/>) was applied to the 3D high-resolution T1WI (Fig 1). As the pulvinar was not identified in this manner, the most representative section was outlined for each patient using a semiautomated contouring technique (Fig 1).<sup>22</sup> The SWI-filtered phase image processing method and reproducibility were discussed in a previous study involving reliable scan-rescan analysis in a subset of 6 patients with MS and 6 healthy volunteers.<sup>5</sup> Voxels having a mean phase value 2 SDs below normal mean phase were identified on a structure-by-structure basis, as previously described, with normal mean phase identified from 330 healthy volunteers aged 8–87 years.<sup>20</sup> The thresholded phase voxels, which were identified as abnormally low, were analyzed to calculate their mean phase, yielding mean phase of the low-phase voxels (MP-LPV).<sup>22</sup>

### Neuropsychological Testing

Neuropsychological testing (NP) was conducted under the supervision of a board-certified neuropsychologist blinded to MR imaging findings. Tests measured processing speed, executive function, and memory in accordance with the recommendations of a consensus panel,<sup>23</sup> and were as follows: oral administration of the Symbol Digit Modalities Test (SDMT)<sup>24</sup> for visual information-processing speed; 3.0-second interval Paced Auditory Serial Addition Test (PASAT)<sup>25</sup> for auditory information-processing speed; the Correct Sorts component of the Delis-Kaplan Executive Function System Sorting Test (DKEFS-CS)<sup>26</sup> for executive function; the Total Learning portion of the second edition of the California Verbal Learning Test (CVLT2)<sup>27</sup> for auditory/verbal learning and memory; and the Total Learning portion of the Brief Visuospatial Memory Test-Revised (BVM-T-R)<sup>28</sup> for visual learning and memory.

### Statistical Analysis

Patients with MS and healthy controls as well as cognitively impaired and nonimpaired patients with MS were compared with

respect to demographic characteristics and MR imaging findings using 1-way ANOVA. *Z* scores were calculated for each NP test based on healthy controls.<sup>29</sup> Impairment was defined as either: a *z* score < -2 on 1 test with a *z* score of < -1.5 on at least 1 other test; a *z* score of < -1.5 on at least 3 tests, as previously defined.<sup>30</sup> In patients with MS, age and years of education were correlated with some NP test scores (SDMT, PASAT, DKEFS-CS, CVLT2); therefore, NP tests were compared between patients with MS and healthy controls using 1-way ANCOVA controlling for age and years of education. Partial correlations controlling for age and years of education assessed the association between NP tests and individual DGM structure volumes, disease duration, and duration of disease-modifying therapy. Pearson correlations were examined between MP-LPV and structure volume and LPV volume. Partial correlations controlling for LPV volume, age, and years of education were examined between NP tests and MP-LPV for individual structures of the DGM. Structures that had the strongest relationship of MP-LPV to NP test performance were included in hierarchical linear regression analyses controlling for age and years of education (in Block 1), followed by LPV volume of the structure in Block 2, MP-LPV of the structure in Block 3, and total tissue volume of the structure in Block 4. In this manner, we assessed the association between iron deposition and cognition, and then reassessed the association while controlling for the effects of atrophy. Tests were considered significant at  $P < .05$ . Analyses were conducted using SPSS for Windows, version 20.0 (IBM, Armonk, New York).

### RESULTS

As expected, patients with MS were significantly more cognitively impaired and performed significantly worse on cognitive tests compared with healthy controls (Table 1). MP-LPV was significantly lower in patients with MS in the thalamus, caudate nucleus, and pulvinar, whereas a statistical trend was found for the putamen ( $P = .085$ ) and globus pallidus ( $P = .051$ ) (Table 1). Age, education, and MP-LPV did not significantly differ between cognitively impaired patients with MS and nonimpaired patients with MS, but duration of disease did ( $P = .009$ ). Except for the globus pallidus with CVLT2, all individual structure volumes were significantly correlated to NP test scores (Table 2). Duration of disease and duration of disease-modifying therapy were not related to NP test scores, and were not further investigated.

Next, we assessed whether MP-LPV was linearly related to cognitive performance in patients with MS. To account for the possibility that tissue atrophy results in tissue loss specifically in regions of low-phase value, thereby potentially altering distribution of iron accumulation, we chose to control for the LPV volume. Controlling for LPV volume, MP-LPV of the caudate nucleus, putamen, globus pallidus, and pulvinar, but not the thalamus, correlated with multiple NP test results (Table 2).

MP-LPV was positively correlated with total volume in the same structure in the caudate and pulvinar, and there was a trend with the putamen ( $P = .075$ ), indicating that as iron accumulation increases, the structure decreases in size. MP-LPV was negatively correlated with LPV volume in the same structure in the putamen, globus pallidus, and pulvinar, indicating that as iron accumulation increases, the voxels that contain abnormally high

**Table 2: Partial correlation of structure volume and mean phase of the low-phase voxels to neuropsychological tests in patients with multiple sclerosis**

	SDMT		PASAT		DKEFS-CS		CVLT2		BVMT-R	
	<i>r</i>	<i>P</i>	<i>r</i>	<i>P</i>	<i>r</i>	<i>P</i>	<i>r</i>	<i>P</i>	<i>r</i>	<i>P</i>
Volume <sup>a</sup>										
Thalamus	0.548	<.001	0.354	.001	0.422	<.001	0.313	.004	0.415	<.001
Caudate nucleus	0.470	<.001	0.357	.001	0.409	<.001	0.257	.019	0.348	.001
Putamen	0.516	<.001	0.405	<.001	0.429	<.001	0.382	<.001	0.518	<.001
Globus pallidus	0.449	<.001	0.296	.007	0.348	.001	NS		0.282	.010
Pulvinar	0.279	.011	0.275	.012	0.309	.005	0.221	.044	0.327	.003
MP-LPV <sup>b</sup>										
Caudate nucleus	0.240	.030	0.232	.036	NS		NS		NS	
Putamen	0.368	.001	NS		0.252	.022	NS		0.238	.031
Globus pallidus	NS		NS		NS		NS		0.235	.033
Pulvinar	0.244	.027	NS		0.255	.021	NS		0.251	.023

**Note:**—NS indicates not significant.

<sup>a</sup> Controlling for age and education.

<sup>b</sup> Controlling for age, education, and low-phase voxel volume.

**Table 3: Mean phase of the low-phase voxels correlated with structure volume and with low-phase voxel volume**

	Volume		LPV Volume	
	<i>r</i>	<i>P</i>	<i>r</i>	<i>P</i>
Caudate nucleus	0.268	.013	NS	
Putamen	NS		−0.502	<.001
Globus pallidus	−0.452	<.001	−0.483	<.001
Pulvinar	0.266	.014	−0.659	<.001

**Note:**—NS indicates not significant.

iron accumulation decrease in collective volume in those structures (Table 3).

Finally, we investigated whether iron-sensitive metrics would have a significant bearing on cognitive function relative to age, education, and volumes of the DGM structures showing a significant correlation between MP-LPV and cognition. The  $R^2$  and  $P$  values of each regression model are reported in Table 4. With the exception of the caudate nucleus for the PASAT, MP-LPV (controlling for LPV volume) added significant variance in the regression models predicting performance score. However, volume of the structure improved all of the models, except for DKEFS-CS and BVMT-R, as predicted by MP-LPV of the pulvinar. Moreover, when a second series of regression models was conducted with structure volume entered ahead of the iron metrics, MP-LPV was not statistically significant. Furthermore, when a third series of regression models was conducted with T2 lesion volume entered along with age and education, none of the other MR imaging measures remained statistically significant.

## DISCUSSION

This study demonstrated a correlation between iron accumulation, as measured by SWI-filtered phase, and cognition in MS. We found that MP-LPV is decreased among patients with MS in the thalamus, caudate nucleus, and pulvinar, and there is a decreasing trend, indicative of higher iron content, in the putamen and globus pallidus. In addition, MP-LPV of the pulvinar, caudate nucleus, putamen, and globus pallidus, but not the thalamus as a whole, is related to cognitive performance. Whereas the correlation between MP-LPV and cognition is statistically significant, the effect size is modest and smaller than the volume/cognition correlation in the DGM. In regression models predicting NP tests, total structural volume significantly increased the  $R^2$  after MP-LPV, whereas entering structure volume first in the models erased

the clinical significance of MP-LPV. We therefore conclude that the association between iron accumulation and cognitive impairment is significant, but considerably smaller than with DGM atrophy or T2 lesion volume.

Previous studies examining cognition in MS have used other methods of investigating iron. An increase in  $R2^*$  rate, indicative of iron, in the basal ganglia, but not the thalamus, of patients with MS correlated with a combined standardized score of the SDMT and PASAT.<sup>31</sup> T2 hypointensity, indicative of iron, in the globus pallidus and caudate nucleus of patients with MS correlated with performance on the SDMT.<sup>32</sup> Similar to our findings, these studies showed correlations between iron and cognition in the DGM; however their correlations were stronger, with  $r$  values in the 0.3–0.6 range. The effects of  $R2^*$ , however, may be hidden by local increases in water content,<sup>33</sup> and T2 relaxation times are more variable in older subjects,<sup>34</sup> making SWI a preferable measure of iron. Magnetic field correlation, another MR imaging method unaffected by dipolar relaxation which is used for iron imaging, found that iron in the thalamus correlated with CVLT2, and that neither the globus pallidus nor the putamen were correlated to SDMT or CVLT2,<sup>35</sup> which contrasts with our findings. Sensitivity to magnetic field inhomogeneities with differing length scales may help explain why these methods yield disparate results.<sup>36</sup>

While the observation of MR imaging phase value as an interpretation of iron concentration is increasingly common, it does not differentiate between iron that is shielded or unshielded, intracellular or extracellular. If iron accumulation is not properly shielded, oxidative stress could lead to necrosis of the cells within its immediate vicinity.<sup>3</sup> As suggested by Kovtunovych et al,<sup>37</sup> with macrophages releasing iron into both spleen tissue and circulation, focal iron deposits in the DGM could disperse within the focal area and out into surrounding tissue upon cell death. By definition, MP-LPV is a measurement in the voxels of the highest iron concentration; its value may be attenuated if iron dissipates as a structure atrophies, thereby masking its association with cognitive performance. We controlled for this confound by making use of the LPV volume as a covariate in our analysis.



**Table 4: Summary of hierarchical linear regressions predicting neuropsychological test scores**

NP Test	Independent Variable (Final Standardized Beta, P Value)	R <sup>2</sup>	R <sup>2</sup> Change	Model P Value	F Change	F Change P Value
SDMT						
Block 1	Age (-0.115, .238), Ed (0.146, .125)	0.064	0.064	.068	2.780	NS
Block 2	Putamen LPV volume (0.012, .929)	0.082	0.018	.074	1.609	NS
Block 3	Putamen MP-LPV (0.154, .241)	0.206	0.124	.001	12.515	.001
Block 4	Putamen volume (0.468, <.001)	0.333	0.127	<.001	15.028	<.001
PASAT						
Block 1	Age (0.112, .318), Ed (0.175, .096)	0.033	0.033	.255	1.388	NS
Block 2	Caudate n. LPV volume (0.009, .941)	0.042	0.010	.318	0.806	NS
Block 3	Caudate n. MP-LPV (0.120, .304)	0.094	0.052	.092	4.564	.036
Block 4	Caudate n. volume (0.319, .009)	0.169	0.075	.011	7.093	.009
DKEFS-CS						
Block 1	Age (-0.081, .444), Ed (0.191, .078)	0.058	0.058	.085	2.544	NS
Block 2	Pulvinar LPV volume (0.161, .365)	0.072	0.013	.109	1.142	NS
Block 3	Pulvinar MP-LPV (0.160, .373)	0.132	0.061	.022	5.577	.021
Block 4	Pulvinar volume (0.214, .123)	0.158	0.026	.017	2.43	NS
CVLT2						
Block 1	Age (-0.207, .049), Ed (0.158, .122)	0.093	0.093	.018	4.212	.018
Block 2	Putamen LPV volume (0.066, .661)	0.133	0.040	.009	3.710	NS
Block 3	Putamen MP-LPV (0.019, .894)	0.164	0.031	.006	2.942	NS
Block 4	Putamen volume (0.333, .012)	0.228	0.064	.001	6.589	.012
BVMT-R						
Block 1	Age (-0.144, .175), Ed (0.083, .437)	0.042	0.042	.172	1.798	NS
Block 2	Pulvinar LPV volume (0.221, .213)	0.076	0.034	.092	2.981	NS
Block 3	Pulvinar MP-LPV (0.146, .413)	0.134	0.058	.02	5.365	.023
Block 4	Pulvinar volume (0.222, .109)	0.162	0.028	.014	2.625	NS

**Note:**—Ed indicates education; n, nucleus; NS, not significant.

With the exception of the thalamus, most of the DGM structures examined had MP-LPV values that positively correlated with structure volume and negatively correlated with LPV volume. We would expect MP-LPV to be positively correlated with structure volume if focal deposits of iron accumulation were connected to atrophy. MP-LPV in the globus pallidus, however, negatively correlated with structure volume, which could indicate a curiously different role for iron in that structure. Meanwhile, MP-LPV was conspicuously higher in the thalamus compared with other structures examined, possibly reflective of different functions of the thalamus. The caudate and putamen together make the striatum of the basal ganglia, a region receiving signals from the sensorimotor, premotor, motor, and prefrontal cortices involving voluntary movement.<sup>38</sup> Meanwhile, the pulvinar receives signals from the visual cortex involving visual attention.<sup>39</sup> Several of the NP tests used manual movement (DKEFS-CS, BVMT-R) and visual perception (SDMT, DKEFS-CS, BVMT-R), likely taxing these structures.

This study is limited by the cross-sectional design, which makes it difficult to characterize the effects of iron in disease course and whether it impacts or is impacted by atrophy. A longitudinal study should help elucidate the temporal and spatial relationships between high iron concentration and tissue atrophy. It also is important to note that the pulvinar structure was analyzed using a single-section method and semiautomated contouring technique, which potentially introduces more variance than analysis using FMRIB's Integrated Registration and Segmentation Tool.

## CONCLUSIONS

High iron deposition, as measured by mean phase of the low-phase voxels, in pulvinar, putamen, caudate nucleus, and globus

pallidus is correlated with cognitive performance in patients with MS. However, the contribution of structure volume is more robust. Longitudinal investigation is underway that may tease apart the temporal evolution of iron deposition and atrophy in MS.

**Disclosures:** Robert Zivadinov—*UNRELATED*: receives personal compensation from Teva Pharmaceuticals, Biogen Idec, EMD Serono, Novartis, Claret, and Sanofi-Genzyme for speaking and consultant fees, and receives financial support for research activities from Biogen Idec, Teva Pharmaceuticals, EMD Serono, Novartis, and Sanofi-Genzyme. Michael Dwyer—*UNRELATED*: received consulting fees from EMD Serono for scientific advisory board activities, and from Claret Medical for image analysis consulting. Ralph H.B. Benedict—*UNRELATED*: receives research support from Accordia, Novartis, Genzyme, Biogen Idec, and Questcor Pharmaceuticals, is on the speakers' bureau for EMD Serono (designing CME courses), and consults for Biogen Idec, Genentech, and Novartis. Dr. Benedict also receives royalties for Psychological Assessment Resources.

## REFERENCES

1. Craelius W, Migdal MW, Luessenhop CP, et al. **Iron deposits surrounding multiple sclerosis plaques.** *Arch Pathol Lab Med* 1982;106:397-99
2. LeVine SM, Lynch SG, Ou CN, et al. **Ferritin, transferrin and iron concentrations in the cerebrospinal fluid of multiple sclerosis patients.** *Brain Res* 1999;821:511-15
3. Williams R, Buchheit CL, Berman NE, et al. **Pathogenic implications of iron accumulation in multiple sclerosis.** *J Neurochem* 2012;120:7-25
4. Haacke EM, Xu Y, Cheng YC, et al. **Susceptibility weighted imaging (SWI).** *Magn Reson Med* 2004;52:612-18
5. Zivadinov R, Heininen-Brown M, Schirda CV, et al. **Abnormal subcortical deep-gray matter susceptibility-weighted imaging filtered phase measurements in patients with multiple sclerosis: a case-control study.** *Neuroimage* 2012;59:331-39
6. Hagemeyer J, Weinstock-Guttman B, Bergsland N, et al. **Iron deposition on SWI-filtered phase in the subcortical deep gray matter of patients with clinically isolated syndrome may precede structure-specific atrophy.** *AJNR Am J Neuroradiol* 2012;33:1596-601

7. Hagemeyer J, Yeh EA, Brown MH, et al. **Iron content of the pulvinar nucleus of the thalamus is increased in adolescent multiple sclerosis.** *Mult Scler* 2013;19:567–76
8. Al-Radaideh AM, Wharton SJ, Lim SY, et al. **Increased iron accumulation occurs in the earliest stages of demyelinating disease: an ultra-high field susceptibility mapping study in clinically isolated syndrome.** *Mult Scler* 2013;19:896–903
9. Zivadinov R, Sepcic J, Nasuelli D, et al. **A longitudinal study of brain atrophy and cognitive disturbances in the early phase of relapsing-remitting multiple sclerosis.** *J Neurol Neurosurg Psychiatry* 2001;70:773–80
10. Benedict RH, Weinstock-Guttman B, Fishman I, et al. **Prediction of neuropsychological impairment in multiple sclerosis: comparison of conventional magnetic resonance imaging measures of atrophy and lesion burden.** *Arch Neurol* 2004;61:226–30
11. Fisher E, Lee JC, Nakamura K, et al. **Gray matter atrophy in multiple sclerosis: a longitudinal study.** *Ann Neurol* 2008;64:255–65
12. Benedict RH, Schwartz CE, Duberstein P, et al. **Influence of personality on the relationship between gray matter volume and neuropsychiatric symptoms in multiple sclerosis.** *Psychosom Med* 2013;75:253–61
13. Batista S, Zivadinov R, Hoogs M, et al. **Basal ganglia, thalamus and neocortical atrophy predicting slowed cognitive processing in multiple sclerosis.** *J Neurol* 2012;259:139–46
14. Schoonheim MM, Popescu V, Rueda Lopes FC, et al. **Subcortical atrophy and cognition: sex effects in multiple sclerosis.** *Neurology* 2012;79:1754–61
15. Bergsland N, Horakova D, Dwyer MG, et al. **Subcortical and cortical gray matter atrophy in a large sample of patients with clinically isolated syndrome and early relapsing-remitting multiple sclerosis.** *AJNR Am J Neuroradiol* 2012;33:1573–78
16. Aubert-Broche B, Fonov V, Ghassemi R, et al. **Regional brain atrophy in children with multiple sclerosis.** *NeuroImage* 2011;58:409–15
17. Calabrese M, Rinaldi F, Grossi P, et al. **Basal ganglia and frontal/parietal cortical atrophy is associated with fatigue in relapsing-remitting multiple sclerosis.** *Mult Scler* 2010;16:1220–28
18. Hagemeyer J, Weinstock-Guttman B, Heininen-Brown M, et al. **Gray matter SWI-filtered phase and atrophy are linked to disability in MS.** *Front Biosci (Elite Ed)* 2013;5:525–32
19. Polman CH, Reingold SC, Edan G, et al. **Diagnostic criteria for multiple sclerosis: 2005 revisions to the “McDonald Criteria.”** *Ann Neurol* 2005;58:840–46
20. Zivadinov R, Rudick RA, De Masi R, et al. **Effects of IV methylprednisolone on brain atrophy in relapsing-remitting MS.** *Neurology* 2001;57:1239–47
21. Patenaude B, Smith SM, Kennedy DN, et al. **A Bayesian model of shape and appearance for subcortical brain segmentation.** *Neuroimage* 2011;56:907–22
22. Hagemeyer J, Dwyer MG, Bergsland N, et al. **Effect of age on MRI phase behavior in the subcortical deep gray matter of healthy individuals.** *AJNR Am J Neuroradiol* 2013;34:2144–51
23. Benedict RHB, Fischer JS, Archibald CJ, et al. **Minimal neuropsychological assessment of MS patients: a consensus approach.** *Clin Neuropsychol* 2002;16:381–97
24. Smith A. *Symbol Digit Modality Test Manual.* Los Angeles: Western Psychological Services; 1982
25. Gronwall DM. **Paced auditory serial-addition task: a measure of recovery from concussion.** *Percept Mot Skills* 1977;44:367–73
26. Delis DC, Kaplan E, Kramer JH. *Delis-Kaplan Executive Function System (D-KEFS):* New York: Psychological Corporation; 2001
27. Delis DC, Kramer JH., Kaplan E, et al. *California Verbal Learning Test.* 2nd ed. San Antonio: Psychological Corporation; 2000
28. Benedict R. *Brief Visuospatial Memory Test-Revised.* Odessa, Florida: Psychological Assessment Resources; 1997
29. Benedict RH, Cookfair D, Gavett R, et al. **Validity of the minimal assessment of cognitive function in multiple sclerosis (MACFIMS).** *J Int Neuropsychol Soc* 2006;12:549–58
30. Benedict RH, Bruce JM, Dwyer MG, et al. **Neocortical atrophy, third ventricular width, and cognitive dysfunction in multiple sclerosis.** *Arch Neurol* 2006;63:1301–06
31. Khalil M, Langkammer C, Ropele S, et al. **Determinants of brain iron in multiple sclerosis: a quantitative 3T MRI study.** *Neurology* 2011;77:1691–97
32. Brass SD, Benedict RH, Weinstock-Guttman B, et al. **Cognitive impairment is associated with subcortical magnetic resonance imaging grey matter T2 hypointensity in multiple sclerosis.** *Mult Scler* 2006;12:437–44
33. Haacke EM, Miao Y, Liu M, et al. **Correlation of putative iron content as represented by changes in R2\* and phase with age in deep gray matter of healthy adults.** *J Magn Reson Imaging* 2010;32:561–76
34. Schenker C, Meier D, Wichmann W, et al. **Age distribution and iron dependency of the T2 relaxation time in the globus pallidus and putamen.** *Neuroradiology* 1993;35:119–24
35. Ge Y, Jensen J, Lu H, et al. **Quantitative assessment of iron accumulation in the deep gray matter of multiple sclerosis by magnetic field correlation imaging.** *AJNR Am J Neuroradiol* 2007;28:1639–44
36. Hu CJ, Jensen H, Williams K, et al. **Comparison of susceptibility-weighted imaging and magnetic field correlation imaging.** *Proc Int Soc Mag Reson Med* 2009;17:4524
37. Kovtunovych G, Eckhaus MA, Ghosh MC, et al. **Dysfunction of the heme recycling system in heme oxygenase 1-deficient mice: effects on macrophage viability and tissue iron distribution.** *Blood* 2010;116:6054–62
38. Arnsten AF, Rubia K. **Neurobiological circuits regulating attention, cognitive control, motivation, and emotion: disruptions in neurodevelopmental psychiatric disorders.** *J Am Acad Child Adolesc Psychiatry* 2012;51:356–67
39. Cotton PL, Smith AT. **Contralateral visual hemifield representations in the human pulvinar nucleus.** *J Neurophysiol* 2007;98:1600–09